Environ. Sci. Technol. **2006**, *40,* 6085−6090

Effect of Particle Age (Fe^0 Content) and Solution pH On NZVI Reactivity: H_2 Evolution and TCE Dechlorination

YUEQIANG LIU AND
GREGORY V. LOWRY*

Department of Civil and Environmental Engineering, Carnegie Mellon University, Pittsburgh, Pennsylvania 15213-3890

Subsurface injection of nanoscale zerovalent iron (NZVI) has been used for the in situ remediation of chlorinated solvent plumes and DNAPL source zones. Due to the cost of materials and placement, the efficacy of this approach depends on the NZVI reactivity and longevity, selectivity for the target contaminant relative to nonspecific corrosion to yield H_2, and access to the Fe^0 in the particles. Both the reaction pH and the age of the particles (i.e., Fe^0 content) could affect NZVI reactivity and longevity. Here, the rates of H_2 evolution and trichloroethene (TCE) reduction are measured over the lifetime of the particles and at solution pH ranging from 6.5 to 8.9. Crystalline reactive nanoscale iron particles (RNIP) with different initial Fe^0 weight percent (48%, 36%, 34%, 27%, and 9.6%) but similar specific surface area were studied. At the equilibrium pH for a $Fe(OH)_2/H_2O$ system (pH = 8.9), RNIP exhibited first-order decay for Fe^0 corrosion (H_2 evolution) with respect to Fe^0 content with a Fe^0 half-life time of 90−180 days. A stable surface area-normalized TCE reduction rate constant $1.0 \times 10^{-3} L \cdot hr^{-1} \cdot m^{-2}$ was observed after 20 days and remained constant for 160 days, while the Fe^0 content of the particles decreased by half, suggesting that TCE reduction is zero-order with respect to the Fe^0 content of the particle. Solution pH affected H_2 evolution and TCE reduction to a different extent. Decreasing pH from 8.9 to 6.5 increased the H_2 evolution rate constant 27 fold from 0.008 to 0.22 day^{-1}, but the TCE dechlorination rate constant only doubled. The dissimilarities between the reaction orders of H_2 evolution and TCE dechlorination with respect to both Fe^0 content and H^+ concentration suggest that different rate controlling steps are involved for the reduction reactions.

Introduction

Nanoscale zerovalent iron (NZVI) effectively degrades a large number of chlorinated organic groundwater contaminants (*1*−*6*). The advantages of using NZVI include its high reactivity with chlorinated organics and its potential to be delivered in situ directly to the contaminant. NZVI has been proposed for in situ remediation of dense nonaqueous phase liquid (DNAPL) source zone (*7*−*9*) and chlorinated solvents plumes (*10*, *11*). When it is injected into a groundwater aquifer, the time over which the particles remain reactive (lifetime) and the rate at which they degrade the target contaminants during their lifetime (reactivity) will control the duration between additional injections, if needed, and the site cleanup time. The reactivity of NZVI during the course of its lifetime, and the geochemical conditions (e.g., pH) that may control this, has not been reported. Lifetime long observations of NZVI reactivity will help to develop models for predicting its lifetime and reactivity under field conditions.

The chemistry of dechlorination of chlorinated organics such as trichloroethylene (TCE) by iron metal has been extensively studied (*12*−*15*). Fe^0 can be oxidized by TCE or by H^+, which are competing reactions. The relevant half reactions for TCE and H^+ reduction, and for iron oxidation are given in eqs 1−4.

$$\mathrm{TCE} + n{\cdot}e^- + (n-3){\cdot}\mathrm{H}^+ \rightarrow \text{products} + 3\mathrm{Cl}^- \quad (1)$$

$$\mathrm{H}^+ + \mathrm{e}^- \rightarrow \mathrm{H}^\bullet \rightarrow \frac{1}{2}\mathrm{H}_2 \quad (2)$$

$$\mathrm{Fe}^{2+} + 2\mathrm{e}^- \rightarrow \mathrm{Fe}^0 \quad E_H{}^0 = -0.447\ \mathrm{V} \quad (3)$$

$$\mathrm{Fe_3O_4} + 8\mathrm{H}^+ + 8\mathrm{e}^- \rightarrow 3\mathrm{Fe}^0 + 4\mathrm{H_2O} \qquad E_H{}^0 = -0.085 - 0.0591{\cdot}p\mathrm{H}\ \mathrm{V} \quad (4)$$

The values of n depend on the products formed (*4*). Oxidation of Fe^0 to Fe^{2+} (eq 3) is most often assumed (*2*, *3*, *12*−*15*). However, the Fe^0/Fe_3O_4 couple is more thermodynamically favorable than Fe^0/Fe^{2+} at pH above 6.1 (*16*). Recent evidence suggests that the oxide film formed at the Fe^0/Fe-oxide interface is magnetite under groundwater conditions, with maghemite (Fe_2O_3) existing at the Fe-oxide/water interface (*17*−*19*). Further, magnetite and maghemite were the only oxide phases found in crystalline NZVI particles (Toda Kogyo Corp., Japan) before and after exposure to H_2O or TCE/H_2O solutions (*5*). Fe^0 oxidation to magnetite (eq 4) provides an additional $^2/_3$ mole of electrons per mole of Fe^0 oxidized compared to oxidation to Fe^{2+} (eq 3). For TCE remediation by crystalline NZVI that cannot activate and use dihydrogen, TCE dechlorination (eq 1) is the desired reaction, and the efficiency depends on the rate of TCE dechlorination relative to nonspecific corrosion to yield H_2 (eq 2). H_2 evolution can be significant. For instance, H_2 evolution was reported to account for >80% of Fe^0 utilization at all TCE concentrations for granular iron in column studies (*20*). Both the solution pH (eqs 1 and 2) and the Fe^0 content of the particles (eqs 3 and 4) may affect the rate of H_2 evolution and TCE reduction.

The pH effects on the reactivity of micrometer-scale iron filings and nanoscale iron for reductive dechlorination have been investigated (*6*, *13*, *21*−*24*). For amorphous NZVI synthesized by reduction of dissolved iron using $NaBH_4$ (aq), a linear decrease of the reaction rate constant for chlorinated ethanes over a pH range 6.5−9.0 was observed (*6*). Similar pH effects for crystalline NZVI are expected but have not been reported. A mechanistic explanation of the pH effect on the dechlorination reaction is not available.

The longevity and long-term performance (effect of aging) of micrometer-sized iron filings have been investigated. Column studies (*15*, *25*) showed a significant decline in the dechlorination reactivity over several years and published data by Klausen et al. (*25*) suggest an exponential decay of the TCE reaction rate constant over 3 years. The decline was attributed to an increase in the mass transfer resistance of contaminants due to insoluble Fe-oxides and Fe-(oxy)-hydroxides formed on particle surface, or to porosity loss and decreased access to iron particles in the column. In

* Corresponding author phone: 412-268-2948; fax: 412-268-7813; e-mail: glowry@cmu.edu.

10.1021/es060685o CCC: $33.50
Published on Web 08/30/2006

contrast, long-term batch studies on the corrosion behavior of micrometer-scale iron filings in unbuffered water reported a constant (zero-order) H_2 corrosion rate over a 125−160 day period suggesting that the iron corrosion rate, hence reactivity, is not changing as the iron ages (*26*, *27*).

NZVI and its application for groundwater remediation differ from micrometer-sized iron fillings and its application in two ways. First, NZVI is not used in a permeable reactive barrier (PRB) where the iron mass ratio is typically is 10−50 wt % and the pH of the surrounding fluid is buffered at a pH of 8−9 by the $Fe(OH)_2/H_2O$ (or Fe_3O_4/H_2O) equilibrium. NZVI is typically injected to provide only 0.2−0.5 wt % (pore water basis) so will likely be subject to corrosion at the prevailing near neutral soil pH (*7*). Second, the particles are small (<100 nm) and significant changes in the Fe^0 content of the particles are expected in a short time. Thus, the iron longevity data and mathematical models used to predict iron lifetime under PRB conditions may not be applicable to NZVI.

The small size and high reactivity of NZVI (thus high Fe^0 utilization rate) make it possible to evaluate the rate of H_2 evolution and TCE dechlorination over the lifetime of the NZVI in a reasonable period of time. Schrick et al. estimated a lifetime of 300 days of bimetallic Ni/Fe nanoparticles assuming zero-order H_2 production (*28*). At pH 8−9, complete oxidation of Fe^0 in highly disordered NZVI to form H_2 was observed in just two weeks (*4*), while crystalline NZVI lasted for up to a year (*3*). The corrosion rate and lifetime of crystalline NZVI at environmentally relevant pH values from 6.5−8 have not been investigated.

The objectives of this study are to determine the H_2 evolution and TCE dechlorination reaction rate and order with respect to the Fe^0 content and solution pH. Crystalline NZVI particles with different Fe^0 content were obtained by drying particles taken from a slurry after different exposure times. The specific surface area and Fe^0 content of the particles were determined by Brunauer−Emmett−Teller (BET) adsorption/desorption method and acid digestion, respectively. The rate of H_2 evolution and TCE dechlorination afforded over the lifetime of the particles was measured. To determine the reaction order with respect to Fe^0, the reactivity of NZVI having different Fe^0 contents was determined at a fixed pH. To determine the reaction order with respect to solution pH, the reactivity of NZVI having the same Fe^0 content was measured at different solution pH. The rate controlling steps for TCE reduction and H_2 evolution by NZVI are postulated based on the observed reaction rates and orders.

Materials and Methods

Chemicals. TCE (99.5+%), cis-1,2-dichloroethylene(c-DCE) (98%), trans-1,2-dichloroethylene(t-DCE) (98%), and 1,1-dichloroethylene(1,1-DCE) (99%) were from Aldrich. A biological buffer 4-(2-hydroxyethyl)piperazine-1-ethansulfonic acid (HEPES, 99%) was from ACROS. Methanol (histological grade) was from Acros. Olefin standards (1000 ppm of ethylene, propene, butene, pentene, hexene), paraffin standards (1020 ppm of methane, ethane, propane, butane, pentane, hexane), acetylene (1000 ppm and 1%), ethylene (1%), ethane (1%), vinyl chloride (VC) (10 ppm), and hydrogen (1.08%) were from Alltech. The balance of each gas standard was N_2 and all reported concentrations are ±2% of the reported concentration. Ultrahigh purity argon, hydrogen (5.18%), and N_2 were from Butler Gas products (Pittsburgh, PA).

Particle Preparation and Characterization. The NZVI used here was reactive nanoscale iron particles (RNIP) supplied by Toda Kogyo Corp., Japan. Particles were shipped and stored in 300 g/L aqueous slurry (pH > 10.6) under anaerobic conditions. Particles were removed from the slurry at different times over a 2-year period and dried after methanol washing (glovebox airlock vacuum, 22 °C) or without washing (oven 105 °C in N_2 at 1 atm). Methanol washing and drying was faster than drying the aqueous slurry directly, but there were no differences in particle reactivity from these two methods. Removing particles at different times provided samples with different Fe^0 content. Dried particles were stored in a glovebox (argon). The N_2 BET-specific surface area was measured using a Tristar 3000 (Micromeritics) BET-surface area analyzer. The Fe^0 content of each sample was determined using acid digestion followed by H_2 quantification, as described previously (*3*). Acid digestion in 1 M HCl for 20 days was sufficient to ensure complete dissolution of the particles.

Batch Reactions. Batch experiments were conducted in 160 mL serum bottles capped by Teflon Mininert valves. Each contained 100 mL of deoxygenated water, 60 mL of headspace, and a weighed mass of RNIP. All reactors were prepared in the anaerobic glovebox so the reactor headspace was initially filled with argon. A saturated TCE solution (1100 mg/L) was added to provide the desired initial TCE concentration. The reactors were rotated on an end-over-end rotator at 30 rpm at 23 ± 2 °C. All reactions were run with excess iron (TCE concentration ~0.04 mM and Fe^0 > 0.86 mM). In control experiments without RNIP, it was demonstrated that TCE loss by mechanisms other than degradation by Fe^0 was negligible (e.g., photodegradation, adsorption, leakage). Mass transfer resistance at the vapor/liquid interface was not considered as these phases are assumed to be in equilibrium.

In reactors without buffer, the solution pH was titrated to 8.9 (the stable pH in NZVI/H_2O system, refer to Figure SI-1 in the Supporting Information) using 10 mM NaOH prior to adding RNIP. After adding RNIP (total particle mass 2 g/L), the reactors were equilibrated 30 min before adding TCE. For long-term studies (~8 months), the reactivity of RNIP with TCE was determined periodically by spiking TCE and monitoring its disappearance and reaction products formed. Before each new TCE spike, the H_2 concentration in the reactor headspace was measured by GC/TCD and then purged with argon. The Fe^0 content of RNIP at each re-spike was calculated from the H_2 produced and TCE degraded assuming $Fe^0 \rightarrow Fe_3O_4$.

To evaluate the effect of pH on H_2 production and TCE reaction rate, 50mM HEPES buffer ($pK_a = 7.5$) was used for pH control. In total, six pH values were evaluated; 6.5, 7, 7.5, 8, 8.5, and 8.9. Each reactor was titrated by adding 1 M NaOH to reach the target pH ± 0.02 pH units. The final pH of reactors after reaction for pH 6.5 and 7.0 was 6.5 and 7.05 indicating that 50mM HEPES provided effective pH control for the conditions in this study.

Analytical. A 100 μL headspace sample was withdrawn from reactors and analyzed for TCE and its products using a 30 m GSQ PLOT capillary column on a HP 6890 GC/FID or H_2 using GC/TCD as described in ref *3*. The H_2 evolution rates and TCE transformation rates of NZVI were evaluated using a kinetic modeling software package, Scientist, v.2.01 (Micromath, St. Louis, MO). For TCE kinetics, the loss of TCE and formation of products were fit concurrently. Reaction pathways previously proposed for RNIP (*4*) were used. Errors reported for the observed reaction rate constants are 95% confidence intervals for the data fits.

H_2 Evolution and TCE Dechlorination Model at Low TCE Concentration. Ignoring competition for reactive sites, a simple mathematical model is hypothesized for H_2 evolution, TCE reduction, and Fe^0 loss. RNIP (~100 nm) has a core/shell structure (*4*, *5*), where the core is Fe^0 and the shell is magnetite/maghemite (*18*). During iron oxidation by TCE or H^+, the Fe^0 core shrinks while the Fe-oxide shell becomes thicker (no significant particle size change was observed after 30 days of reaction and >50% Fe^0 loss (*4*)). Assuming

reduction of H^+ or TCE at the oxide surface, it is reasonable to hypothesize that the reaction rate of TCE and H^+ will be a function of the particle surface area, Fe^0 content, and the solution H^+ concentration (pH).

$$\frac{dH_2}{dt} = k_{H_2} \cdot [SA] \cdot [Fe^0]^a \cdot [H^+]^b \quad (5)$$

$$\frac{dC_{TCE}}{dt} = -k_{TCE} \cdot C_{TCE} \cdot [SA] \cdot [Fe^0]^x \cdot [H^+]^y \quad (6)$$

In eqs 5−6, k_{H2} is the H_2 evolution rate constant and k_{TCE} is the TCE reaction rate constant, $[Fe^0]$ is the particle Fe^0 content, $[H^+]$ is the H^+ concentration, and [SA] is the surface area concentration (m^2/g), C_{TCE} is TCE concentration, and a and b and x and y are the reaction orders with respect to Fe^0 content and H^+ concentration for H_2 evolution and TCE reduction, respectively. In a system containing only TCE and H^+ as potential oxidants, and assuming that Fe^0 is oxidized to Fe_3O_4, the Fe^0 content of the particles can be determined according to the reaction stoichiometry, where n is defined in eq 1.

$$\frac{dFe^0}{dt} = -\frac{3}{4}k_{H_2} \cdot [SA] \cdot [Fe^0]^a \cdot [H^+]^b - \frac{3n}{8}k_{TCE} \cdot C_{TCE} \cdot [SA] \cdot [Fe^0]^x \cdot [H^+]^y \quad (7)$$

Results and Discussion

Particle Characterization. The RNIP Fe^0 content ranged from 48 ± 0.2 wt % for the freshest particles (19 days in slurry prior to drying) to 9.6 ± 0.4 wt % for the most oxidized particles (210 days in slurry prior to drying). For convenience, RNIP is designated according to its Fe^0 content, e.g., Fe48% contains 48 wt % Fe^0 prior to reaction. The N_2 BET specific surface area for all of the samples were 10 ± 2 m^2/g, even though they had been exposed to water for times ranging from a few days to a few months. This suggests that the particle surfaces are not changing significantly during oxidation in water and is consistent with the hypothesized model that the Fe^0 core shrinks while the magnetite shell grows at the Fe^0/Fe_3O_4 interface. All reported TCE reaction rate constants are normalized by the measured N_2 BET specific surface area of 10 m^2/g.

Fe^0 Decay and H_2 Evolution Rate and Reaction Order with Respect to Fe^0 Content. The Fe^0 content of RNIP as a function of time in a concentrated (300 g/L) slurry at pH 10.6 is shown in Figure 1a. Freshly made particles are designed to have ~70 wt % Fe^0 and ~30 wt % Fe_3O_4. The Fe^0 content decreased exponentially over 2 years of exposure to water with $k_{obs,\ Fe0} = 6.0 \pm 2.1 \times 10^{-3}$ day^{-1}. This corresponds to a Fe^0 half-life time of 90−180 days in solution at pH 10.6. Note that removing the last point (t = 730 days) does not significantly affect the fit ($k_{obs,\ Fe0} = 6.0 \pm 2.3 \times 10^{-3}$ day^{-1} over the 200 day period).

In the absence of oxidants other than H^+, the rate of the Fe^0 content change can also be determined from the H_2 evolved due to iron corrosion in water assuming $Fe^0 \rightarrow Fe_3O_4$.

$$\frac{d[Fe^0]}{dt} = -\frac{3}{4}\frac{d[H_2]}{dt} \quad (8)$$

A pseudo-first-order rate of H_2 evolution from Fe27% was observed over a 280-day period (Figure 1b). This simple model slightly underestimates H_2 evolution in the early times and slightly overestimates H_2 evolution at later times, suggesting that the rate slows somewhat as the particles age. The reaction rate constant $k_{obs,H2} = 3.1 \pm 1.8 \times 10^{-3}$ day^{-1} and the half-life time ranged from 140 to 530 days. This is contrary to prior

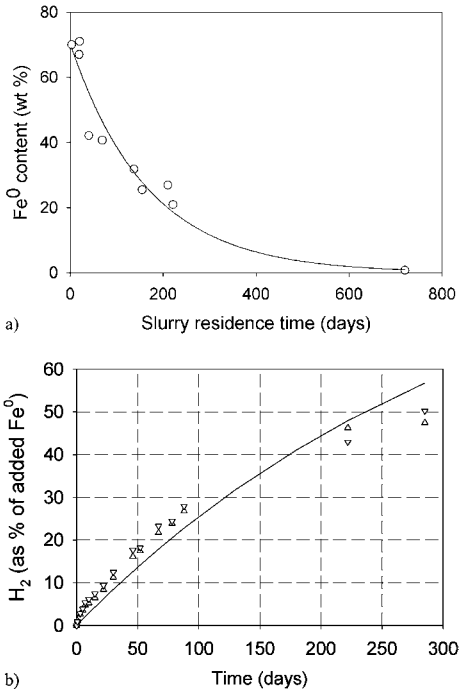

FIGURE 1. (a) Fe^0 content of RNIP removed from the aqueous slurry (300 g/L) at different times. The curve represents first-order data fit (k_{obs} = 0.0060 1/day, r^2 = 0.927). (b) H_2 production from 500 mg/L Fe27% RNIP; data are from duplicate reactors. The curve represents the first-order data fit ($k_{obs,H2}$ = 0.0031 1/day, r^2 = 0.972).

reports of constant (zero order) H_2 evolution rates from micrometer-sized iron filings measured over similar time periods (*26*, *28*). The disparity between RNIP and iron fillings is likely due to their different particle size. For iron fillings, there is excess Fe^0 and the Fe^0 content of the particles is not changing appreciably during the measurements. For RNIP, the Fe^0 content is changing over the course of the measurement. To further verify the assumption of first-order H_2 evolution with respect to Fe^0 content, H_2 evolution from RNIP with different initial Fe^0 content was measured under the same conditions as for Fe27%, but for a shorter time (22 days). The initial H_2 evolution rate was proportional to the initial Fe^0 content (Figure SI-2, Supporting Information), supporting the first-order reaction for H_2 evolution with respect to Fe^0 content (a = 1 in eq 5).

TCE Reaction Rate and Order with Respect to Fe^0 Content. To determine the effect of aging (Fe^0 content) on RNIP reactivity with TCE, the TCE dechlorination rate was measured periodically while RNIP aged in water for 230 days. The TCE reduction rate was determined 8 or 9 times during the 230 day period by spiking TCE (0.04 mM) and monitoring its degradation over a 3−4 day period. A carbon mass balance of 90−110% was obtained for each spike. Typical data for TCE dechlorination are provided in the Supporting Information (Figure SI-3). The Fe^0 content at each spike was calculated from the H_2 that had evolved and TCE that had degraded up to that point. The Fe^0 content and $k_{obs,\ TCE}$ values for Fe48% and Fe9.6% are plotted in Figure 2a. Fe36% and Fe34% were not included for clarity, but these showed similar behavior and are provided in Supporting Information Figure SI-4.

In all cases, there was a significant decrease in the observed TCE reaction rate constants during the first 7−10 days, e.g., $k_{obs,TCE}$ for Fe48% decreased from 6.2×10^{-3} L·hr^{-1}·m^{-2} to 1.0 $\times 10^{-3}$ L·hr^{-1}·m^{-2} after 10 days, followed by a constant or slightly increasing rate constant during which time the Fe^0 content of the particles decreased by ~40%. For Fe9.6%, reactivity with TCE and H_2 evolution ceased after 170 days when the Fe^0 content reached ~4.6%. Focusing on the long

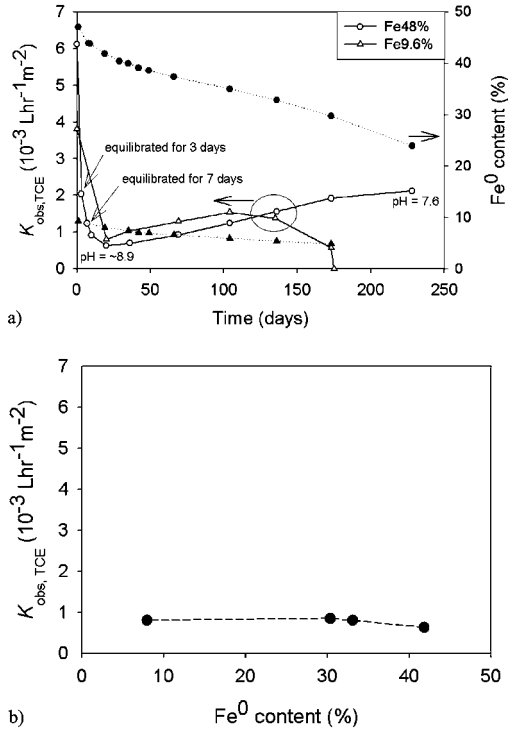

FIGURE 2. (a) Fe^0 content and surface area normalized TCE reaction rate constants ($k_{obs,\ TCE}$, L hr^{-1} m^{-2}) over the lifetime of Fe48% and Fe9.6% without buffer (initial pH 8.9, final pH 6.9−7.6). RNIP concentration is 2 g/L. Filled symbols are Fe^0 content and open symbols are surface area normalized observed reaction rate constants ($k_{obs,TCE}$). Points labeled at t = 3 and 7 days were equilibrated without TCE prior to determining $k_{obs,TCE}$. (b) The TCE reaction rate constants ($k_{obs,\ TCE}$) for each Fe^0 content measured at 20 days when the transient period has ended. Lines in Figure 2 are interpolated (not fit) and only meant to guide the eye.

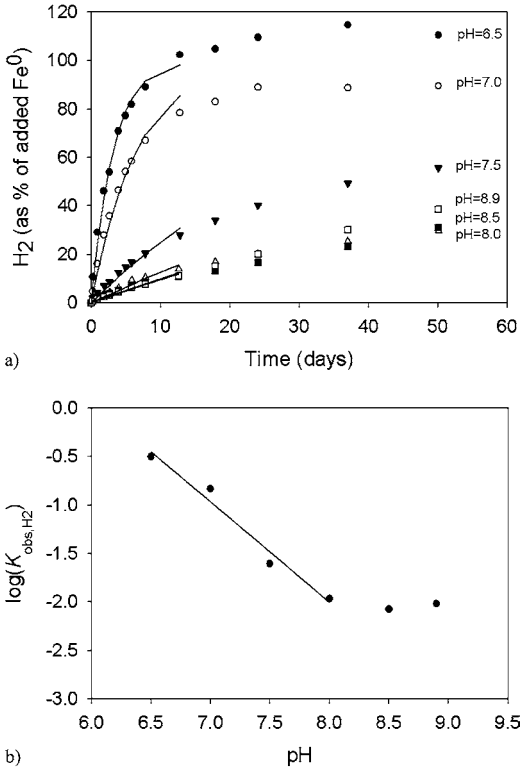

FIGURE 3. (a) H_2 evolution from 300 mg/L Fe9.6% at different pH in 50 mM HEPES buffer. The curves represent the pseudo-first-order fit of H_2 evolution in the first 13 days at each pH. (b) Log of the H_2 evolution rate constant ($k_{obs,\ H2}k_{H2}$·[SA]·[H$^+$]^y) vs pH. Line is linear fit of the data below pH 8.5, with a slope −1.03 and regression r^2 0.974.

term behavior (t > 10 days), these results suggest the following. First, $k_{obs,TCE}$ is not decreasing appreciably as the Fe^0 content of RNIP decreases during aging in water. The moderate increase in k_{obs} over the 7 month period is due to a decrease in the reactor pH from 8.9 initially to 6.9 at t = 170 days for Fe9.6% (and from 8.9 to 7.6 at 230 days for Fe48%) due to the reduction of TCE and formation of HCl. (The pH effect on $k_{obs,TCE}$ is discussed below). Second, RNIP continues to degrade TCE until the Fe^0 content reaches <5% indicating that nearly all of the Fe^0 is utilized. The relatively constant $k_{obs,TCE}$ over the life of the particles suggests that the reaction with TCE is essentially zero order with respect to Fe^0. Further evidence supporting the conclusion that the TCE reaction is zero-order with respect to Fe^0 content is that the reaction rate constants for RNIP at day 20 with presumably similar solution pHs are nearly the same regardless of the Fe^0 content (Figure 2b).

Even though the long term behavior of RNIP is the most relevant for field application, the transient behavior at t < 10 days merits some attention. The rapid decline in $k_{obs,TCE}$ over the first 10 days appears to be due to particle equilibration with water rather than to exposure to TCE. The $k_{obs,TCE}$ for RNIP Fe48% that had been exposed to water (without TCE) for 3 and 7 days prior to reactivity testing followed the trend of gradually decreasing rate constants (Figure 2a). One possible explanation for the transient behavior is that highly reactive defects (pits and cracks) may have formed on surface of the particles during drying (*29*). TCE reduction reactions occurring at the defects (pits and cracks) are faster than through the magnetite shell (*30*, *31*). Once the reactivity of these defect sites decreases due to corrosion and formation of the magnetite shell, the TCE reaction rate constant stabilizes for the remainder of the life of the particle. This is corroborated by the similarity between the stable reaction rate constants observed after the transient period for dried particles (0.7−2.1 × 10^{-3} L·hr^{-1}·m^{-2}), and those for RNIP taken directly from a slurry that had not been dried (1.8−3.5 × 10^{-3} L·hr^{-1}·m^{-2}).

H_2 Evolution Rate and Reaction Order with Respect to [H$^+$]. The H_2 evolution from Fe9.6% at different pH (6.5, 7.0, 7.5, 8.0, 8.5, and 8.9) was measured over 50 days (Figure 3a). At pH 8.9, HEPES buffer (50mM) used to control pH did not affect the H_2 evolution rate relative to that measured at pH 8.9 without HEPES (data not shown) so the buffer effect, if any, is assumed to be small. The H_2 evolution was pseudo-first-order with respect to Fe^0 content and the rate increased with decreasing pH between pH 6.5−8.0, but increases above pH 8 had little effect. In each case, the % recovery is calculated assuming Fe^0 → Fe_3O_4. For pH 6.5 and 7.0 (Figure 3a), enough time had elapsed to allow complete oxidation of the Fe^0 in RNIP. The difference between the recovery at pH 6.5 and 7.0 (≈100% at pH 6.5, ≈85% recovery at pH 7) suggests that different Fe-oxide phases (e.g., Fe_3O_4 or green rust (*17*−*19*)) may be forming at different pHs. A closer examination of the Fe-oxides formed as a function of pH is warranted given its potential impact on the reducing power of NZVI, but is outside of the scope of the present study, and this uncertainty does not change the conclusions of this study.

A pseudo-first-order fit of H_2 evolution is shown in Figure 3a. After 13 days, the Fe^0 was completely consumed at pH 6.5 so the fits were made based on data collected in the first 13 days in order to compare the initial rates for each pH. The log $k_{obs,H2}$ vs pH is shown in Figure 3b. Using values between pH 6.5−8.0 where pH had an effect on the H_2 evolution rate constant, the coefficient b in eq 5 is 1.03, indicating first-order H_2 production with respect to [H$^+$] over the pH range

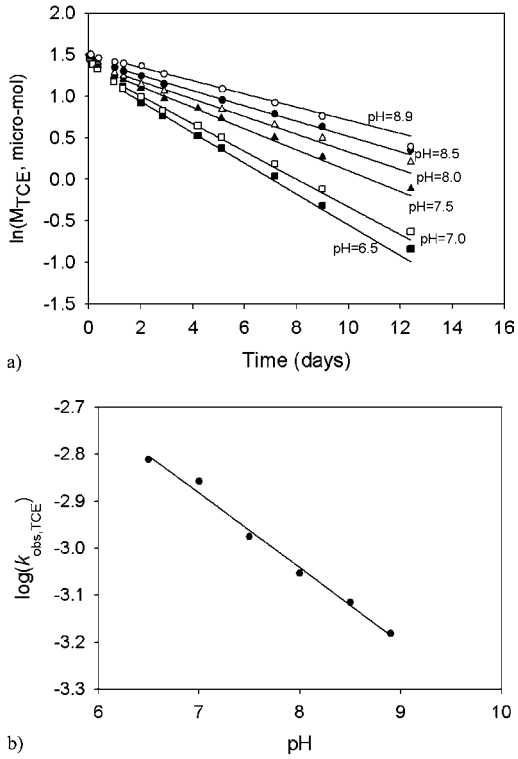

FIGURE 4. (a) TCE reaction rate constant ($k_{obs,\,TCE}k_{TCE}$·[SA]·[H^+]^y) for 500 mg/L Fe9.6% at different pH in 50 mM HEPES buffer. Lines are pseudo-first-order fit for TCE loss at each pH. (b) TCE reaction rate constant vs pH. Line represents the linear fit of data, with a slope 0.16 and regression r^2 0.990.

observed at most groundwater sites (pH 6.5−8). The shift from first-order with respect to [H^+] to zero order at pH > 8 is unclear, but suggests that H^+ is no longer involved in the rate controlling step for H_2 evolution at pH > 8.

TCE Reaction Rate and Order with Respect to [H^+]. TCE degradation by Fe9.6% was measured at pH 6.5, 7.0, 7.5, 8.0, 8.5, and 8.9 (Figure 4a). Decreasing pH from 8.9 to 6.5 resulted in a doubling of the observed TCE reaction rate constant, which is an order of magnitude less than the increase for k_{H2} over the same pH range. A linear relationship between the logarithm of reaction rate constant and pH was obtained (Figure 4b). A coefficient $y = 0.16$ ($R^2 = 0.9898$) in eq 6 indicates a weak dependence on pH and that H^+ is not a dominant part of the rate-limiting step of TCE dechlorination by RNIP. This is consistent with that reported by Matheson and Tratnyek (1994) for carbon tetrachloride dechlorination by micrometer-sized iron filings (*13*), and suggests that RNIP behaves similarly to micrometer-scale iron filings. And the result is consistent with Song and Carraway (2005) who reported that the rate constants for reduction of chlorinated ethanes by $NaBH_4$ synthesized NZVI varied less than an order of magnitude from pH 9.0 to 6.5 (*6*).

Mechanistic Understanding of the Different Reaction Orders for the H_2 Evolution and TCE Reduction Reactions. Based on the results of this study, between pH 6.5 and 8, H_2 evolution by RNIP is pseudo-first-order with respect to both the Fe^0 content and [H^+] ($a = b = 1$ in eq 5), while TCE reduction by RNIP is near zero order with respect to the Fe^0 content, and of order 0.16 with respect to [H^+] ($x \approx 0$ and $y = 0.16$ in eq 6). The difference between the reaction orders for H_2 evolution and TCE dechlorination with respect to Fe^0 content and [H^+] can be attributed to differences in the rate controlling steps for each reaction. Both H_2 evolution and TCE reduction require protons (H atoms) and electrons. It is reasonable to assume that the availability of electrons is proportional to the Fe^0 content of RNIP. H_2 evolution is represented by eq 10, where protons and electrons (Fe^0) are required to form adsorbed H atoms (k_1). Two adsorbed H atoms can combine to form H_2 (k_2).

$$2Fe + 2H^+ + 2e^- \xrightarrow{k_1} 2Fe - H^\bullet \xrightarrow{k_2} 2Fe + H_2 \quad (10)$$

For H_2 evolution the first-order dependence on Fe^0 content and H^+ indicates that $k_2 \gg k_1$ and that formation of adsorbed H species is the rate controlling step for H_2 evolution. This agrees with published reports for hydrogen evolution at near neutral pH where k_1 has been shown to be the rate controlling step (*32*, *33*). TCE reduction requires that TCE adsorb to the iron surface, and that TCE reduction occur via direct electron transfer or via adsorbed H. Both reduction mechanisms would be a function of the availability of electrons, i.e., Fe^0 content. Reduction by adsorbed H would also be a function of pH. The weak dependence of the TCE dechlorination rate on both Fe^0 content and H^+ implies that chemical or physical factors other than electron transfer are controlling the rate of TCE reduction.

Implication for In Situ NZVI Application. The corrosion rate of the Fe^0 in NZVI is an important consideration for storage, shipping, and the reducing power of the NZVI injected into the ground. Even at high pH > 10, there is a slow decay of the Fe^0 in the particles. Based on the results of this study, changes in the Fe^0 content will not appreciably change its reactivity with the target contaminant such as TCE, but it will have less reducing capacity than fresh particles with higher Fe^0 content and should be considered in the economics of NZVI application. The accumulation of pressurized H_2 in sealed containers over extended times may pose potential explosion risk. The storage and transport of concentrated NZVI suspensions in nonreactive solvents, e.g., polyethylene glycol, followed by dilution with H_2O just prior to injection should be considered if other properties such as dispersion stability are not adversely affected.

The high buffer capacity of most soil implies that there will be little pH change with a typical injection amount of NZVI (<0.5%, (*7*)). The rapid H_2 evolution observed at neutral pH will greatly affect the lifetime of NZVI, and may significantly affect the NZVI dose needed to achieve remediation goals. This is especially true if NZVI is used for plume treatment where target contaminant concentrations are low, and if the evolved H_2 cannot be utilized downgradient by microorganisms that can also degrade the target contaminant. At neutral pH, the reduction capacity of NZVI would be utilized in just a few weeks, and additional injections would be needed compared to application where pH is 8.0 or greater. Ensuring that NZVI is injected at or very near the source area where contaminant concentrations are high (>10 mg/L for TCE) may help mitigate this problem as increased contaminant concentrations have been shown to reduce the amount of H_2 evolved (*3*, *4*).

The consistent H_2 evolution from RNIP over its lifetime implies the potential for enhanced bioremediation for TCE removal by acting as long-term H_2 source. H_2 is the preferred electron donor for microorganisms that biodegrade chlorinated solvents (*34*). Based on the H_2 evolution rates determined in this study, an injected amount yielding 0.5 wt % (the upper application dose) RNIP to uncontaminated soil, i.e., no oxidants other than H^+, the H_2 evolved in the injection area could exceed the solubility of H_2 (~800 μM at STP) and outgas. In addition, the H_2 concentration in the treatment zone, and for a distance downgradient of 3−5 times the length of the treatment zone would be substantially higher than is optimal for dehalorespiring bacteria which would participate in the degradation of TCE (*35*) (model assumptions and results provided in the Supporting Information). However,

inhibited H_2 evolution from RNIP due to the presence of high concentration TCE (DNAPL) (*4*) or other competing oxidants (e.g., NO_3^-) may provide a much lower steady-state H_2 concentration that is suitable for biodegradation of dissolved TCE near or downgradient from the source zone. The potential for combining in situ abiotic remediation of the source zone with enhanced bioremediation of the downgradient plume may be possible and could further increase the attractiveness of NAVI as a DNAPL source-zone treatment alternative.

Acknowledgments

This research was funded in part by the Office of Science (BER), U.S. Department of Energy (DE-FG07-02ER63507), the U.S. EPA (R830898), the NSF (CTS-0521721), and SERDP (W912HQ-06-C-0038). Any opinions, findings, and conclusions or recommendations expressed in this material are those of the authors and do not necessarily reflect the views of the U.S. EPA or the U.S. Department of Energy. We thank Prof. Greg Rohrer (Material Science and Engineering, CMU) for the use of his GC/TCD, and the WaterQUEST center at CMU for laboratory equipment and maintenance support.

Supporting Information Available

pH evolution in an RNIP/water system, initial H_2 evolution rates of RNIP with different initial Fe^0 content, typical TCE reduction and product formation by RNIP, $k_{obs,\ TCE}$ for Fe36% and Fe34%, and simulated H_2 evolution in a sandy aquifer. This material is available free of charge via the Internet at http://pubs.acs.org.

Literature Cited

(1) Wang, C. B.; Zhang, W. X. Synthesizing nanoscale iron particles for rapid and complete dechlorination of TCE and PCBs. *Environ. Sci. Technol.* **1997**, *31*, 2154−2156.
(2) Zhang, W. Nanoscale iron particles for environmental remediation: An overview. *J. Nanopart. Res.* **2003**, *5*, 323−332.
(3) Liu, Y.; Choi, H.; Dionysiou, D.; Lowry, G. V. Trichloroethene hydrodechlorination in water by highly disordered monometallic nanoiron. *Chem. Mater.* **2005**, *17*, 5315−5322.
(4) Liu, Y.; Majetich, S. A.; Tilton, R. D.; Sholl, D. S.; Lowry, G. V. TCE. dechlorination rates, pathways, and efficiency of nanoscale iron particles with different properties. *Environ. Sci. Technol.* **2005**, *39*, 1338−1345.
(5) Nurmi, J. T.; Tratnyek, P. G.; Sarathy, V.; Baer, D. R.; Amonette, J. E.; Pecher, K.; Wang, C.; Linehan, J. C.; Matson, D. W.; Penn, R. L.; Driessen, M. D. Characterization and properties of metallic iron nanoparticles: spectroscopy, electrochemistry, and kinetics. *Environ. Sci. Technol.* **2005**, *39*, 1221−1230.
(6) Song, H.; Carraway, E. R. Reductive of chlorinated ethanes by nanosized zero-valent iron: kinetics, pathways, and effects of reaction conditions. *Environ. Sci. Technol.* **2005**, *39*, 6237−6245.
(7) Gavaskar, A.; Tatar, L.; Condit, W. *Cost and performance report: nanoscale zero-valent iron technologies for source remediation*, Naval Facilities Engineering Service Center: Port Hueneme, CA, **2005**.
(8) Quinn, J.; Geiger, C.; Clausen, C.; Brooks, K.; Coon, C.; O'Hara, S.; Krug, T.; Major, D.; Yoon, W.-S.; Gavaskar, A.; Holdsworth, T. Field demonstration of DNAPL dehalogenation using emulsified zero-valent iron. *Environ. Sci. Technol.* **2005**, *39*, 1309−1318.
(9) Saleh, N.; Phenrat, T.; Sirk, K.; Dufour, B.; Ok, J.; Sarbu, T.; Matyjaszewski, K.; Tilton, R. D.; Lowry, G. V. Adsorbed triblock copolymers deliver reactive iron nanoparticles to the oil/water interface. *Nano Lett.* **2005**, *5*, 2489−2494.
(10) Elliott, D. W.; Zhang, W. Field assessment of nanoscale bimetallic particles for groundwater treatment. *Environ. Sci. Technol.* **2001**, *35*, 4922−4926.
(11) Schrick, B.; Hydutsky, B. W.; Blough, J. L.; Mallouk, T. E. Delivery vehicles for zerovalent metal nanoparticles in soil and groundwater. *Chem. Mater.* **2004**, *16*, 2187−2193.
(12) Gillham, R. W.; F., O. H. S. Enhanced degradation of halogenated aliphatics by zero-valent iron. *Ground Water* **1994**, *32*, 958−967.
(13) Matheson, L. J.; Tratnyek, P. G. Reductive dehalogenation of chlorinated methanes by iron metal. *Environ. Sci. Technol.* **1994**, *28*, 2045−2053.
(14) Orth, W. S.; Gillham, R. W. Dechlorination of trichloroethene in aqueous solution using Fe0. *Environ. Sci. Technol.* **1996**, *30*, 66−71.
(15) Farrell, J.; Kason, M.; Melitas, N.; Li, T. Investigation of the long-term performance of zero-valent iron for reductive dechlorination of trichloroethylene. *Environ. Sci. Technol.* **2000**, *34*, 514−521.
(16) Pourbaix, M. J. N. *Atlas of electrochemical equilibria in aqueous solutions*; Pergamon Press: New York, 1966.
(17) Ritter, K.; Odziemkowski, M. S.; Gillham, R. W. An in situ study of the role of surface films on granular iron in the permeable iron wall technology. *J. Contam. Hydrol.* **2002**, *55*, 87−111.
(18) Odziemkowski, M. S.; Simpraga, R. P. Distribution of oxides on iron materials used for remediation of organic groundwater contaminants−Implications for hydrogen evolution reactions. *Can. J. Chem.* **2004**, *82*, 1495−1506.
(19) Kohn, T.; Livi, K. J. T.; Roberts, A. L.; Vikesland, P. J. Longevity of granular iron in groundwater treatment processes: corrosion product development. *Environ. Sci. Technol.* **2005**, *39*, 2867−2879.
(20) Farrell, J.; Melitas, N.; kason, M.; Li, T. Electrochemical and column investigation of iron-mediated reductive dechlorination of trichloroethylene and perchloroethylene. *Environ. Sci. Technol.* **2000**, *34*, 2549−2556.
(21) Tamara, M. L.; Butler, E. C. Effects of iron purity and groundwater characteristics on the rate and products in degradation of carbon tetrachloride by iron metal. *Environ. Sci. Technol.* **2004**, *38*, 1866−1876.
(22) Chen, J.-L.; Al-Abet, S. R.; Ryan, J. A.; Li, Z. Effects of pH on dechlorination of trichloroethylene by zero-valent iron. *J. Hazard. Mater.* **2001**, *B83*, 243−254.
(23) Li, T.; Farrell, J. Reductive dechlorination of trichloroethene and carbon tetrachloride using iron and palladized-iron cathodes. *Environ. Sci. Technol.* **2000**, *34*, 173−179.
(24) Deng, B.; Burris, D. R.; Campbell, T. J. Reductive of vinyl chloride in metallic iron-water systems. *Environ. Sci. Technol.* **1999**, *33*, 2651−2656.
(25) Klausen, J.; Vikesland, P. J.; Kohn, T.; Burris, D. R.; Ball, W. P.; Roberts, A. L. Longevity of granular iron in groundwater treatment processes: solution composition effects on reduction of organohalides and nitroaromatic compounds. *Environ. Sci. Technol.* **2003**, *37*, 1208−1218.
(26) Reardon, E. J. Zerovalent iron: styles of corrosion and inorganic control on hydrogen pressure buildup. *Environ. Sci. Technol.* **2005**, *39*, 7311−7317.
(27) Reardon, E. J. Anaerobic corrosion of granular iron: measurement and interpretation of hydrogen evolution rates. *Environ. Sci. Technol.* **1995**, *29*, 2936−2945.
(28) Schrick, B.; Blough, J. L.; Jones, A. D.; Mallouk, T. E. Hydrodechlorination of trichloroethylene to hydrocarbons using bimetallic nickle-iron nanoparticles. *Chem. Mater.* **2002**, *14*, 5140−5147.
(29) Ryan, M. R.; Williams, D. E.; Chater, R. J.; Hutton, B. M.; McPhail, D. S. Why stainless steel corrodes. *Nature* **2002**, *415*, 770−774.
(30) Gotpagar, J.; Lyuksyutov, S.; Cohn, R.; Grulke, E.; Bhattacharyya, D. Reductive dehologenation of trichloroethylene with zero-valent iron: surface profiling microscopy and rate enhancement studies. *Langmuir* **1999**, *15*, 8412−8420.
(31) Gaspar, D. J.; Lea, A. S.; Engelhard, M. H.; Baer, D. R. Evidence for localization of reaction upon reduction of carbon tetrachloride by granular iron. *Langmuir* **2002**, *18*, 7688−7693.
(32) Bockris, J. O.; Carbajal, J. L.; Scharifker, B. R.; Chandrasekaran, K. Adsorbed hydrogen on iron in the electrochemical reduction of protons−an FTIR study. *J. Electrochem. Soc.* **1987**, *134*, 1957−1963.
(33) Wang, J.; Farrell, J. Investigating the role of atomic hydrogen on chloroethene reactions with iron using Tafel analysis and electrochemical impedance spectroscopy. *Environ. Sci. Technol.* **2003**, *37*, 3891−3896.
(34) Seshadri, R.; Adrian, L.; Fouts, D. E.; Eisen, J. A. Genome sequence of the PCE-dechlorinating bacterium dehalococcoides ethenogenes. *Science* **2005**, *307*, 105−108.
(35) Yang, Y.; McCarty, P. L. Competition for hydrogen within a chlorinated solvent dehalogenating anaerobic mixed culture. *Environ. Sci. Technol.* **1998**, *32*, 3591−3597.

Received for review March 22, 2006. Revised manuscript received July 11, 2006. Accepted July 21, 2006.

ES060685O